

# COMPRESSIVE SENSING FOR OVER-THE-AIR ULTRASOUND

*Petros Boufounos*

Mitsubishi Electric Research Laboratories  
Cambridge, MA 02139,  
*petrosb@merl.com*

## ABSTRACT

The advent of Compressive Sensing has provided significant mathematical tools to enhance the sensing capabilities of hardware devices. In this paper we apply Compressive Sensing to improve over-the-air ultrasonic sensing capabilities. We demonstrate that using an appropriate scene model it is possible to pose three-dimensional surface reconstruction of a scene as a sparse recovery problem. By transmitting incoherent wideband ultrasonic pulses and receiving their reflections a sensor array can sense the scene and reconstruct it using standard CS reconstruction algorithms. We further demonstrate that it is possible to construct virtual arrays that exploit the sensors' motion. Thus we can obtain three-dimensional scene reconstruction using a linear mobile array.

*Index Terms*— Compressed Sensing, Ultrasonic transducer arrays, Ultrasonic imaging

## 1. INTRODUCTION

Ultrasonic transducers are ubiquitous inexpensive sensing devices with wide applications in medical imaging, material testing, underwater acoustics and communications, and over-the-air distance sensing and ranging. Over-the-air applications, in particular, are numerous and include automotive sensing for parking and lane change assistance, indoor robotic navigation, localization of beacons, and object distance estimation.

Current sensing approaches use narrowband ultrasonic sensors, operating independently or in a phased array configurations. Simple ranging estimation is usually performed by transmitting an ultrasonic pulse and determining the time-of-flight to reach the nearest object and return to the transducer by computing a simple cross-correlation of the transmitted and the received signal. More challenging localization applications use a steerable phased array of sensors to scan the scene for the target and its distance [1].

In this paper we demonstrate how Compressive Sensing—a very powerful recently emerged signal acquisition paradigm—can be exploited to significantly improve ultrasonic sensing capabilities. Specifically, we demonstrate that using wideband incoherent pulses, separate for each transmitter, it is possible to obtain a very accurate three-dimensional reconstruction of the sensed scene. In addition, we illustrate how a synthetic array can be constructed to exploit the motion of a physical array. Although we present the results in the context of ultrasonic sensing, some of the principles and the algorithms we describe are immediately applicable to other phased array processing and radar applications.

The paper is organized as follows. The next section provides some background on Compressive Sensing. Section 3 describes a typical ultrasonic sensing system, the corresponding sensing and scene model and the model for a synthetic array. The models are

used in Sec. 4 to formulate the recovery problem and the pulse design problem. We verify our results experimentally in Section 5.

## 2. COMPRESSIVE SENSING BACKGROUND

Compressive Sensing (CS) is a recently emerged field in signal processing that enables signal acquisition using very few measurements compared to the signal dimension, as long as the signal is sparse in some basis [2–5]. Using CS, a signal  $\mathbf{x} \in \mathbb{C}^N$  with only  $K$  non-zero coefficients can be recovered from only  $M = O(K \log(N/K))$  linear non-adaptive measurements, compactly represented using

$$\mathbf{y} = \mathbf{A}\mathbf{x}, \mathbf{y} \in \mathbb{C}^M, \quad (1)$$

where  $\mathbf{A} \in \mathbb{C}^{M \times N}$  is the measurement matrix, modeling the measurement system. To be able to recover all  $K$ -sparse signals  $\mathbf{x}$ , it is necessary that  $\mathbf{A}$  does not map two distinct  $K$ -sparse signals to the same measurement vector, i.e., that for all  $K$ -sparse vectors  $\mathbf{x}_1 \neq \mathbf{x}_2$

$$\mathbf{A}\mathbf{x}_1 - \mathbf{A}\mathbf{x}_2 = \mathbf{A}(\mathbf{x}_1 - \mathbf{x}_2) \neq \mathbf{0}. \quad (2)$$

Assuming (2), we can recover  $\mathbf{x}$  by solving

$$\hat{\mathbf{x}} = \arg \min_{\mathbf{x} \in \mathbb{C}^N} \|\mathbf{x}\|_0 \text{ subject to } \mathbf{y} = \mathbf{A}\mathbf{x}, \quad (3)$$

where the  $\|\cdot\|_0$  counts the number of non-zero coefficients. This is an NP-hard problem in general and becomes infeasible in high dimensions.

Computationally efficient exact signal recovery can be guaranteed if  $\mathbf{A}$  obeys a restricted isometry property (RIP) of order  $2K$ , i.e., if there is a universal constant  $\delta_{2K}$  such that for all  $2K$ -sparse  $\mathbf{z}$

$$(1 - \delta_{2K})\|\mathbf{z}\|_2^2 \leq \|\mathbf{A}\mathbf{z}\|_2^2 \leq (1 + \delta_{2K})\|\mathbf{z}\|_2^2. \quad (4)$$

If  $\mathbf{A}$  has a small RIP constant  $\delta_{2k}$ , it approximately maintains  $\ell_2$  distances between  $K$ -sparse signals. In addition to efficient exact recovery, the RIP guarantees robustness to measurement noise and robustness to deviation from the strictly sparse signal model. Although verifying the RIP also has combinatorial complexity, a surprising result is that random matrices with a sufficient number of rows can achieve small coherence and small RIP constants with overwhelming probability [5].

There are two fundamental approaches to reconstruction from CS measurements: convex optimization and greedy search algorithms. If the measurement matrix obeys the RIP with sufficiently small constant  $\delta_{2K}$  and there is no measurement noise, it is possible to exactly recover signals from the measurement vector  $\mathbf{y}$  using the convex optimization [5]

$$\hat{\mathbf{x}} = \arg \min_{\mathbf{x} \in \mathbb{C}^N} \|\mathbf{x}\|_1 \text{ subject to } \mathbf{y} = \mathbf{A}\mathbf{x}. \quad (5)$$

The RIP further guarantees robustness to noise and stable recovery of compressible signals. Similarly, the RIP guarantees that greedy sparse reconstruction algorithms—originating with the Matching Pursuit [6]—robustly recover the signal. A recently emerged body of literature provides a variety of greedy algorithms with such guarantees, of which the Compressive Sampling Matching Pursuit (CoSaMP) [7] and the Subspace Pursuit [8] are the most recent examples.

### 3. ULTRASONIC SCENE SENSING

#### 3.1. System Description

A general ultrasonic sensing system consists of a number of transmitters and receivers arranged in some configuration in space. An example is shown in Fig. 1. The  $S$  transmitters, depicted in green triangles, transmit wide-band ultrasonic pulses which are reflected from the objects in the scene and received by the  $L$  receivers, depicted in blue circles. In practice, the transmitters and the receivers might be the same device (transducer), operating in different mode during pulse transmission and reception.

The scene to be sensed is a three dimensional volume containing several objects. The scene can be analyzed by discretizing the volume into  $N = N_x \times N_y \times N_z$  small volumes (voxels). Using  $n = 1, \dots, N$  to linearly index these voxels, the reflectivity of each voxel is denoted using  $x_n$ . The reflectivity of each voxel is a non-zero complex number if the volume corresponding to that voxel is not empty and the voxel is not occluded by objects between the voxel and the sensors. The reflectivity of the voxel is zero if it is empty or if it is occluded from the sensors by another nonempty voxel. Thus only the surface of each object facing the sensor array can be sensed since the remaining object volume is occluded from the sensor array. Our analysis ignores the effect of partial occlusions, i.e. voxels that are occluded only for some of the sensors. The effect of partial occlusions in practice is small compared to the overall precision of the ultrasonic sensing system.

#### 3.2. Scene Measurement

Since the transducers are wideband, each of them emits a wide bandwidth of frequencies. The signal  $p_s(t)$  emitted by each of the transducers can be represented by its discrete-time samples at the Nyquist rate  $f_o$  (i.e., twice the signal bandwidth, corresponding to period  $T_o = 1/f_o$ ). This representation is very useful for digital signal generation and processing. Thus, the discrete-time signal  $p_s[m] = p_s(mT_o)$  emitted by transmitter  $s$  can be decomposed to a sum of discrete frequency tones using the discrete Fourier transform (DFT):

$$p_s[m] = \sum_f P_{s,f} e^{-j\omega_f m}, \quad s = 1, \dots, S, \quad f = 1, \dots, F, \quad (6)$$

where  $P_{k,f}$  are the DFT coefficients of  $p_k$ , and  $\omega_f = 2\pi f/F$  is the angular frequency of the corresponding tone.

Similarly the recorded signal at receiver  $l$ ,  $r_l(t)$  can be sampled using  $r_l[m] = r_l(mT)$  and decomposed using the DFT:

$$r_l[m] = \sum_f R_{l,f} e^{-j\omega_f m}, \quad l = 1, \dots, L, \quad f = 1, \dots, F, \quad (7)$$

where  $R_{l,f}$  are the DFT coefficients of  $r_l$ .

Every voxel in the scene reflects the wideband ultrasonic pulse received by each transmitter according to the voxel's reflectivity  $x_n$ . Letting  $d_{s,n}$  be the distance from transmitter  $k$  to voxel  $n$  and  $d_{n,l}$  be

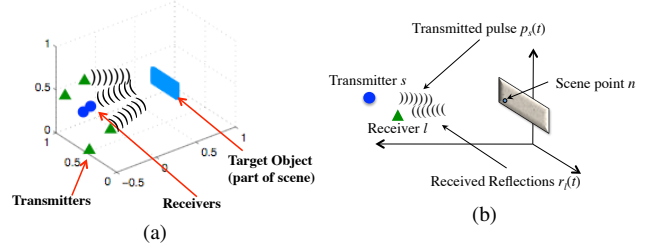


Fig. 1. Ultrasonic Sensing System

the distance from voxel  $n$  to receiver  $l$ , the total path of an ultrasonic pulse through voxel  $n$  is  $d_{s,l,n} = d_{s,n} + d_{n,l}$ . Thus the total delay from the transmission of the pulse until the reception is  $d_{s,l,n}/c$ , where  $c$  is the speed of sound in air (or in the medium in which the device operates). In terms of samples,  $\tau_{s,l,n} = d_{s,l,n}/cT$ .

Each receiver receives the sum of all the pulses transmitted from all the transmitters as reflected from all the voxels. Thus, the DFT coefficients for receiver  $l$  are as follows:

$$R_{l,f} = \sum_n \left( \sum_s P_{s,f} e^{-j\omega_f \tau_{s,l,n}} \right) x_n, \quad (8)$$

By stacking in one vector all the received frequency components from all the receivers, the system can be described using the following sensing equation:

$$\mathbf{r} = \mathbf{A}\mathbf{x}, \quad (9)$$

$$\mathbf{r} = [R_{1,1} \dots R_{1,F} \dots R_{L,1} \dots R_{L,F}]^T$$

$$\mathbf{x} = [x_1 \dots x_N]^T$$

$$\mathbf{A} = \begin{bmatrix} \sum_s P_{s,1} e^{-j\omega_1 \tau_{s,1,1}} & \dots & \sum_s P_{s,1} e^{-j\omega_1 \tau_{s,1,N}} \\ \vdots & \ddots & \vdots \\ \sum_s P_{s,F} e^{-j\omega_F \tau_{s,1,1}} & \dots & \sum_s P_{s,F} e^{-j\omega_F \tau_{s,1,N}} \\ \vdots & \ddots & \vdots \\ \sum_s P_{s,1} e^{-j\omega_1 \tau_{s,L,1}} & \dots & \sum_s P_{s,1} e^{-j\omega_1 \tau_{s,L,N}} \\ \vdots & \ddots & \vdots \\ \sum_s P_{s,F} e^{-j\omega_F \tau_{s,L,1}} & \dots & \sum_s P_{s,F} e^{-j\omega_F \tau_{s,L,N}} \end{bmatrix}$$

where  $\mathbf{r}$  denotes the received coefficients vector,  $\mathbf{A}$  the overall transmission operator and  $\mathbf{x}$  the scene reflectivity.

The goal of the recovery algorithm is to undo the action of  $\mathbf{A}$  on  $\mathbf{x}$  and thus recover  $\mathbf{x}$  from the measurements of the received coefficients  $\mathbf{r}$ . Consequently,  $\mathbf{x}$  is the recovered scene.

#### 3.3. Virtual (Synthetic) Array Modeling

The same sensing model can be used to model a synthetic array in which the sensor location changes and separate sets of data are obtained from each location. The combined received data are subsequently used to reconstruct the scene. Thus the synthetic array has significantly improved reconstruction capabilities compared to the actual physical array. This operation is similar to the operation of a synthetic aperture radar (SAR) which exploits the motion of a satellite or an aircraft to image the earth.

The transducers sense (and obtain a snapshot of) the scene from  $Q$  different positions. For each position, a sensing equation similar to (9) can be written:

$$\mathbf{r}_q = \mathbf{A}_q \mathbf{x}, \quad (10)$$

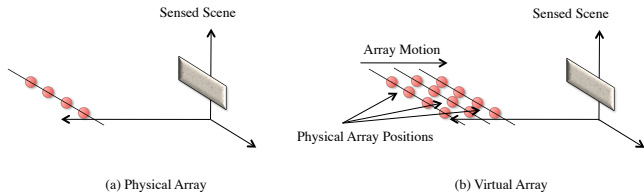


**Fig. 2.** Virtual Array Configuration

where  $\mathbf{r}_q$  is the recorder pulses at the  $q^{th}$  position, and  $\mathbf{A}_q$  is the sensing matrix, as derived by the geometry of the sensors and the scene in the  $q^{th}$  position. Combining the sensing equations from all the positions results to the sensing equation:

$$\begin{bmatrix} \mathbf{r}_1 \\ \vdots \\ \mathbf{r}_Q \end{bmatrix} = \begin{bmatrix} \mathbf{A}_1 \\ \vdots \\ \mathbf{A}_Q \end{bmatrix} \mathbf{x} \quad (11)$$

The computational methods in Sec. 4.1 can subsequently be used to recover  $\mathbf{x}$  from (11), even if recovery from separate snapshots in (10) is not possible.

As an example consider the linear physical array pictured in Fig. 2. Such an array, fundamentally, can only resolve two dimensions: distance from the array and angle to array axis. There is a fundamental rotational ambiguity with axis of rotation the same as the array axis. Still, by translating the array, a two-dimensional virtual array can be generated which does not exhibit the rotational ambiguity. Assuming omnidirectional sensors, the virtual array only exhibits a fundamental mirror ambiguity of which the mirroring plane is the same as the array plane. With directional sensors or different array motion, even this ambiguity can be resolved.

## 4. COMPRESSIVE ULTRASONIC SENSING

### 4.1. Measurement Processing and Scene recovery

The sensing systems described in (9) and (11) are, in general, severely underdetermined systems. The scene size  $N$  will in most cases be significantly larger than the number of possible measurements. Thus, we need to assume that the sensed scene has further structure that we can exploit.

Specifically, we assume the scene is sparse. Since most of the scene is empty or occluded, most of the coefficients  $x_n, n = 1, \dots, N$  are zeros. Therefore, we can safely assume that the vector  $\mathbf{x}$  contains at most  $N_x \times N_z$  non-zero elements, i.e., at most  $1/N_y$  of its coefficients are non-zero. Usually the scene is even sparser in practice.

Recovery of a sparse vector from the measured coefficients  $\mathbf{r}$  is possible using a variety of methods, as described in Sec. 2. One example is a convex optimization formulation, which computes:

$$\hat{\mathbf{x}} = \arg \min_{\mathbf{x}} \|\mathbf{x}\|_1 \text{ such that } \mathbf{r} \approx \mathbf{A}\mathbf{x} \quad (12)$$

$$\text{or } \hat{\mathbf{x}} = \arg \min_{\mathbf{x}} \|\mathbf{x}\|_1 + \lambda \|\mathbf{r} - \mathbf{A}\mathbf{x}\|_2^2, \quad (13)$$

where  $\lambda$  is a regularization parameter [9]. Another example is using a *greedy algorithm* such as matching pursuit (MP), orthogonal matching pursuit (OMP), and CoSaMP [7]. If a model for the scene is known, then model-based reconstruction algorithms can also be used to improve the reconstruction quality [10].

In this work we use CoSaMP as the reconstruction algorithm because of its flexibility and its ability to handle complex arithmetic. Using CoSaMP variations, it is very easy to accommodate scene models, quantization, saturation, and streaming signals, as necessary in the applications of the sensing system. [10–14].

### 4.2. Pulsing Design

Correct sparse recovery of the sensed scene depends on the coherence properties of the sensing matrix  $\mathbf{A}$ . These properties are controlled by the design of the pulses, through their Fourier transform coefficients  $P_{s,f}$ .

To ensure incoherency of the columns of  $\mathbf{A}$  we select all coefficients  $P_{s,f}$  as independent and identically distributed complex random variables. This empirically ensures that the  $S$  pulses are incoherent with each other.

An important parameter that affects our ability to design  $\mathbf{A}$  is the number of degrees of freedom available in the selection of  $P_{s,f}$ . In particular, the duration of the pulse dictates the number of coefficients available when the pulse is sampled at the Nyquist rate, and, therefore, the number of degrees of freedom in the discrete Fourier transform of the signal. For example, a pulse of length  $M$  samples (i.e.,  $MT_o = M/f_o$  seconds) provides  $M$  total real-valued degrees of freedom.

Still not all these parameters are available. In most over-the-air ultrasonic sensing scenarios the part of the spectrum that is audible by humans and some animals should not be used. For example if the available bandwidth is 40-50KHz, only 20% of the degrees of freedom are available. If the available bandwidth is 30-50KHz, 40% of the degrees of freedom are available. For pulse duration  $D$  seconds, and fraction  $b$  of bandwidth utilization, the available degrees of freedom are  $bDf_o$ .

The pulse duration is critical if the same transducers are used both for transmission and reception. In particular, the distance of the closest object in the scene determines the roundtrip time from the instant the pulse starts being transmitted to the instant the pulse returns to the sensor and should be received. If the total pulse duration is longer than the roundtrip time, then the transducer will not have completed the transmission and will not be able to receive part of the reflected signal.

## 5. EXPERIMENTAL RESULTS

To validate our model we performed simulations using both physical and virtual arrays, which we describe below.

Figure 3 demonstrates the simulation results for a physical array with 5 transmitter elements and 3 receiver elements. Figure 3(a) plots the original scene, to be acquired by the array, with the transmitters represented by green triangles and the receivers represented by blue circles. The transducers in the simulation were modeled after the ProWave 400WB160 ceramic transducer, with a bandwidth of  $\sim 15$ KHz [15]. The object colors in the scene represent the reflectivity of each object.

An attempt to reconstruct the scene using least squares estimation, i.e., using

$$\hat{\mathbf{x}} = \mathbf{A}^\dagger \mathbf{y}$$

is demonstrated in Fig. 3(b). Since the system is underdetermined, this approach will produce the least  $\ell_2$ -norm solution of the sensing equation (9). In this attempt there was no noise added to the sensed scene. As expected, least squares reconstruction fails to recover the signal, even with ideal, noiseless acquisition.

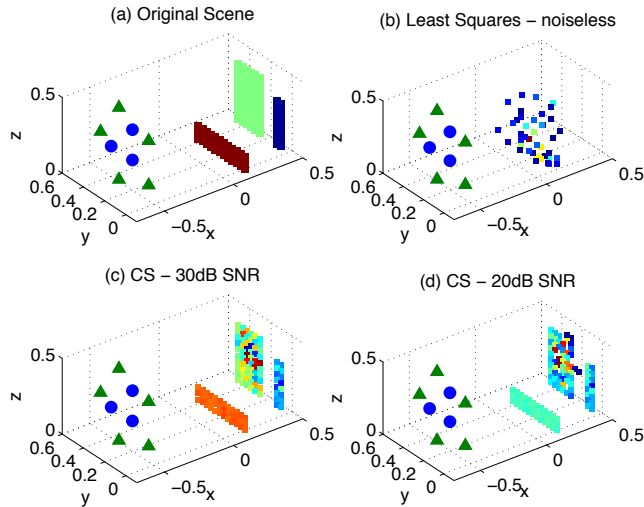


Fig. 3. Static array simulation experiments

Sparse recovery using CoSaMP, as described in this paper, is shown in Figs. 3(c) and (d), for input SNR at 30dB and 20dB, respectively. As shown in the figure, the higher the SNR the better the reconstruction. Most of the error in Fig. 3(d) arises where nearby objects are very close, and, therefore, the ambiguity is high.

One of the key observations in our simulations is that significant diversity (i.e., incoherence of  $\mathbf{A}$ ), and therefore improved reconstruction, can be achieved by increasing the number of transmitters without increasing the number of receivers. This has significant computational advantages since only the number of receivers determines the size of  $\mathbf{A}$ . Of course there are diminishing returns in the benefit of increasing transmitters without simultaneously increasing the number of receivers. The study of this trade-off is the subject of a future publication.

Simulations using a virtual array are shown in Fig. 4. In this simulation a four-element transducer array is positioned in two different locations with different measurements obtained from each location. The transducers operate both as transmitters and as receivers at every location by first transmitting the pulse and then receiving the reflection before moving to the next location. To avoid the fundamental mirror-image ambiguity with respect to the plane of a two dimensional array, as described in Sec. 3.3 the physical array is not linear. The two transducers at the edges are elevated by 10cm compared to the two middle ones. Because of the translation we have 8 effective transmitters and receivers. As evident from Fig. 4(b), we can achieve fairly accurate reconstruction even at 10dB SNR, lower than the simulations above.

The results we present validate our approach and demonstrate that over-the-air ultrasonic sensing can be significantly enhanced using compressive sensing. The model presented is quite powerful and amenable to further refinement, which we defer to future publication. Our initial investigation raises significant questions, such as the optimal array design, and the sensing limits of the system, which we continue to investigate.

## 6. REFERENCES

[1] A. Hernandez, J.P. Derutin, F.J. Alvarez, and A. Jimenez, "Ultrasonic sensory system for mobile robots and autonomous ve-

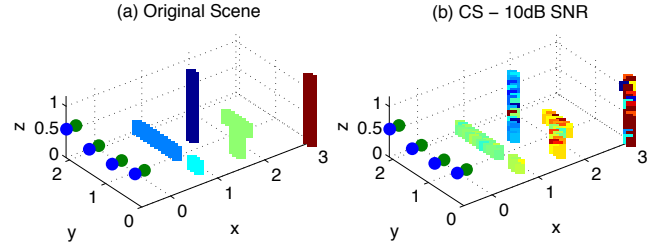


Fig. 4. Virtual array simulation experiments

hicles," in *IEEE International Symposium on Industrial Electronics (ISIE)*, Jun. 2007, pp. 1548–1553.

- [2] E. J. Candès, J. Romberg, and T. Tao, "Robust Uncertainty Principles: Exact Signal Reconstruction from Highly Incomplete Frequency Information," *IEEE Trans. Info. Theory*, vol. 52, no. 2, pp. 489–509, Feb. 2006.
- [3] D. Donoho, "Compressed sensing," *IEEE Trans. Info. Theory*, vol. 52, no. 4, pp. 1289–1306, Sept. 2006.
- [4] E. Candès, J. Romberg, and T. Tao, "Stable Signal Recovery from Incomplete and Inaccurate Measurements," *Comm. Pure and Applied Math.*, vol. 59, no. 8, pp. 1207–1223, Aug. 2006.
- [5] E. J. Candès, "Compressive sampling," in *Proc. International Congress of Mathematicians*, Madrid, Spain, 2006, vol. 3, pp. 1433–1452.
- [6] S. G. Mallat and Z. Zhang, "Matching pursuits with time-frequency dictionaries," *IEEE Trans. Signal Processing*, vol. 41, no. 12, pp. 3397–3415, Dec. 1993.
- [7] D. Needell and J. Tropp, "CoSaMP: Iterative signal recovery from incomplete and inaccurate samples," *Appl. Comput. Harmon. Anal.*, vol. 26, no. 3, pp. 301–321, 2009.
- [8] W. Dai and O. Milenkovic, "Subspace pursuit for compressive sensing signal reconstruction," *IEEE Trans. Inform. Theory*, vol. 55, no. 5, pp. 2230–2249, 2009.
- [9] S. S. Chen, D. L. Donoho, and M. A. Saunders, "Atomic decomposition by basis pursuit," *SIAM J. Scientific Computing*, vol. 20, no. 1, pp. 33–61, 1999.
- [10] R.G. Baraniuk, V. Cevher, M.F. Duarte, and C. Hegde, "Model-based compressive sensing," *Information Theory, IEEE Transactions on*, vol. 56, no. 4, pp. 1982–2001, 2010.
- [11] J. Laska, P. Boufounos, M. Davenport, and R. Baraniuk, "Democracy in action: Quantization, saturation, and compressive sensing," *Preprint*, 2009.
- [12] J. Laska, P. Boufounos, and R. Baraniuk, "Finite-range scalar quantization for compressive sensing," in *Proc. Sampling Theory and Applications (SampTA)*, Marseille, France, May 2009.
- [13] P. Boufounos and M.S. Asif, "Compressive sampling for streaming signals with sparse frequency content," in *44th Annual Conference on Information Sciences and Systems (CISS)*, 2010, pp. 1–6.
- [14] P. Boufounos and M.S. Asif, "Compressive Sensing for Streaming Signals using the Streaming Greedy Pursuit," in *Proc. Military Communications Conference (MILCOM)*, San Jose, CA, Oct. 31–Nov. 3 2010.
- [15] Prowave Ltd., *Air Ultrasonic Ceramic Transducers 400WB160*, 2006.